IGARSS 2023 - 2023 IEEE International Geoscience and Remote Sensing Symposium | 979-8-3503-2010-7/23/$31.00 ©2023 IEEE | DOI: 10.1109/IGARSS52108.2023.10281788

TOWARDS GPS-DENIED SPOTLIGHT SAR IMAGE FORMATION

Andrew Willis, Christopher Beam

University of North Carolina at Charlotte
Dept of Electrical and Computer Engineering
Charlotte, NC 28223-0001
{cbeam18, arwillis}@uncc.edu

Garrett Demeyer, Kevin Brink

Air Force Research Laboratory
Munitions Directorate
Eglin AFB, FL, 32542
{garrett.demeyer.1, kevin.brink} @us.af.mil

ABSTRACT

Synthetic Aperture Radar (SAR) systems emit pulses of (Radio Frequency) RF energy from an antenna into the environment over short intervals in time. Reflected RF energy is received coherently by a receiving antenna and signal processing focusing algorithms process the received signals using one of many potential focusing algorithms to form 2D images of the scene. Formation of these images requires highly accurate knowledge of the antenna state, e.g., the position, orientation and their velocities, when transmitting and receiving RF signals. This information is typically obtained using a combination of a high-quality Global Positioning System (GPS) receiver and a highly-accurate Inertial Navigation System (INS). SAR dependence on GPS and INS data prohibit SAR image formation in GPS-denied contexts which limit the application of this technology. This work investigates approaches for focusing SAR images when GPS is unavailable.

Index Terms— Synthetic Aperture Radar (SAR), Spotlight SAR, Radar signal processing, radar back projection, GPS-denied environments

1. INTRODUCTION

Synthetic Aperture Radar (SAR) systems emit pulses of (Radio Frequency) RF energy from an antenna into the environment over short intervals in time. A receiving RF antenna received the reflected RF energy and signal processing focusing algorithms process the received signals to form 2D images of the scene. Applications of SAR includes target recognition [1, 2], mapping difficult terrain [3], ocean surveillance [4], mapping and tracking geological phenomena [5], and mapping forest cover and biomass [6].

Formation of SAR images requires highly accurate knowledge of the antenna state, i.e., position, orientation and velocity, at the time RF signals are transmitted [7, 8]. This information is typically obtained using a combination of a high-quality Global Positioning System (GPS) receiver and a highly-accurate Inertial Navigation System (INS). SAR dependence on GPS and INS data prohibits SAR image formation in GPS-denied contexts and this restriction limits the application of this technology. This article investigates the theory and methods for focusing SAR images when an absolute position for the antenna, typically provided by via GPS, is unavailable. To do so, we revisit the first-principles of SAR image formation and derive a non-linear algorithm for SAR focusing in GPS-denied contexts.

This article proposes steps that allow the focusing of SAR images in GPS-denied contexts. Contributions of this work include: (1) specification of a canonical coordinate system for processing SAR signals taken from unknown poses, (2) specification of a focusing performance functional sensitive to relative pose error within the canonical coordinate system, and (3) analysis of the sensitivity of the performance functional to pose error to define necessary and sufficient criteria for pose recovery and successful SAR focusing.

We demonstrate our approach for GPS-denied SAR focusing by focusing on real-world SAR data as provided by the GOTCHA data set [9]. Our approach for GPS-denied SAR focusing consists of three steps: (1) choose a model and canonical coordinate system for the unknown vehicle trajectory, (2) construct a likelihood function that detects coherent structure in focused SAR images given a trajectory, and (3) execute a search to find extremes of the likelihood function that correspond to candidate values for the unknown antenna initial poses of the trajectory. Completion of these steps yields estimates for the antenna pose changes for each pulse emitted during the formation of the synthetic aperture.

2. RELATED WORK

Existing work on SAR's sensitivity to motion error exists in [7, 8, 10, 11] which discusses auto focus algorithms. Auto focus algorithms seek to correct motion error to improve SAR image quality. Yet, auto-focus algorithms such as [8, 11] do not address gross, i.e., large-scale, motion errors and are restricted to situations where the approximate trajectory is al-

This research is sponsored by an AFRL/National Research Council fellowship and results are made possible by resources made available from AFRL's Autonomous Vehicles Laboratory at the University of Florida Research Engineering Education Facility (REEF) in Shalimar, FL.

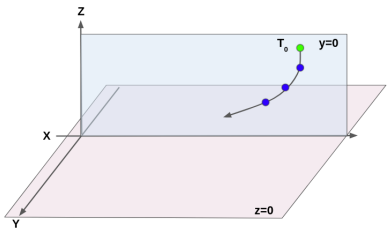

Fig. 1: The canonical coordinate system used for analysis.

ready known within a fraction of the nominal radar wavelength, λ. Specifically, these methods are applicable for relative trajectory corrections on the order of $\sim \frac{\lambda}{20}$ (see [7] p. 48). For many applications, e.g., X-band radar where $\lambda \approx 3cm$. this requires small relative motion errors, $\epsilon < 1 - 2mm$. *As such, existing work does not consider the difficult problem of finding antenna trajectories whose relative pose errors fall into the* $\epsilon > 2mm$ *regime.* Solution for larger errors requires finding a solution to a non-deterministic polynomial-time hard (NP-hard) optimization problem [8] and the computational complexity of solving this problem seems to have deterred the academic community investigating solutions.

3. METHODOLOGY

Vehicle trajectory during the SAR aperture is modeled as N unknown pose changes $\Delta\mathbf{T}_{1,\ldots,N}$ relative to a default initial absolute pose $\mathbf{T}_0$ defined in a canonical coordinate system as seen in Fig. 1 and requires an initial guess for the velocity, v_0, at the initial pose $\mathbf{T}_0$. Our trajectory model is considered to be well-approximated by a smooth 3D curve which allows the trajectory to be modeled as a 3D space-curve model. Our curve model is a parametric 3D space curve $C(X(s), Y(s), Z(s))$ where variation along each coordinate system axis is modeled as a polynomial function of the curve arc length, s, e.g., $X(s) = \Sigma_{k=0}^{K} \alpha_k s^k$. The curve is then sampled to generate a sequence of 3D antenna trajectory pose changes required by the SAR focusing algorithm.

The likelihood of a candidate trajectory being correct is assessed by the performance function. Several performance functions were considered, e.g., image entropy and total variation, and it was found that the SAR image column entropy outperformed other methods for detecting SAR image coherence. The column entropy function calculates the total entropy of the each column in the focused image according to the equation $H(Y|r = r_0) = \sum_{y \in \mathcal{Y}} p(y) \log p(y)$.

4. RESULTS

Our experimental results are broken into 4 parts: 1) Sensitivity to Aperture Initial Pose Errors, 2) Sensitivity to Aperture Pose Change Errors, 3) Necessary Criterion for Searching the Solution Space, 4) Demonstration of a Candidate Solution. Experiments are performed using 400 pulses from the GOTCHA dataset which provides the phase history, antenna frequency, bandwidth, and antenna position data required to focus the phase history into SAR images.

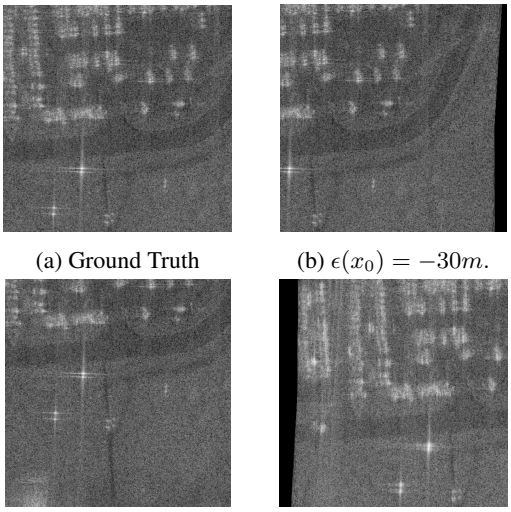

(a) Ground Truth (b) $\epsilon(x_0) = -30m.$

(c) $\epsilon(y_0) = -30m.$ (d) $\epsilon(z_0) = +30m.$

Fig. 2: (a-d) show the impact of initial pose error for the initial pose parameters.

4.1. Sensitivity to $\mathbf{T}_0$ Aperture Initial Pose Errors

Fig. 2 shows results of an experiment using the GOTCHA dataset where absolute motion error have been introduced to the ground truth trajectory. One can see that errors in the initial antenna pose serve to shift the position of the focused target phase center in the SAR image away from the true target phase center, but do not otherwise degrade the quality of the focused SAR image. Experimental results indicate that image quality will remain intact despite large error in the initial pose parameters.

4.2. Sensitivity to $\Delta\mathbf{T}_{1,\ldots,N}$ Aperture Pose Change Errors

Fig. 3 shows results of an experiment using the GOTCHA data set where relative motion errors have been introduced by the addition of Gaussian noise. One can see that small errors, e.g., $\epsilon(x, y, z) = \frac{\lambda}{10}$, in the pose change position parameters cause significant degradation in the focused SAR image. Experimental results indicate that image quality is highly sensitive to errors in the antenna pose change parameters. Specifically, structures are visually evident for values of the error for the regime $E[\epsilon(x, y, z)] = \frac{\lambda}{10}$. This qualitative measure of visual quality provides insight on the "breakdown region" for being able to focus a SAR image.

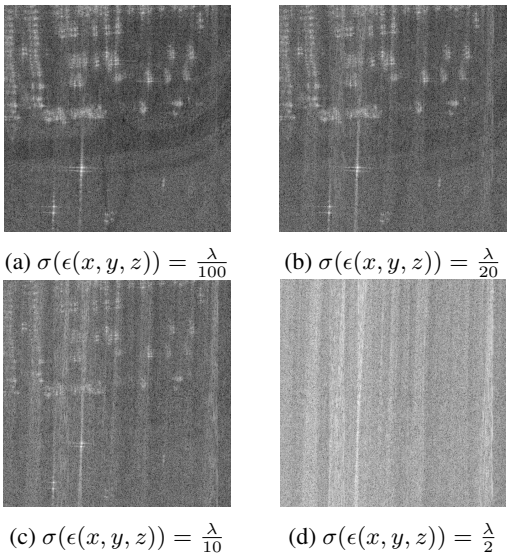

(a) $\sigma(\epsilon(x,y,z)) = \frac{\lambda}{100}$ (b) $\sigma(\epsilon(x,y,z)) = \frac{\lambda}{20}$

(c) $\sigma(\epsilon(x,y,z)) = \frac{\lambda}{10}$ (d) $\sigma(\epsilon(x,y,z)) = \frac{\lambda}{2}$

Fig. 3: (a-d) show the impact of error in pose changes for zero-mean Gaussian noise with increasing variance.

4.3. Necessary Criterion for Searching the Solution Space

Figure 4(a-c) show the error surface geometric structure and numerical behavior for the column entropy performance functional for a collection of trajectories in the vicinity of the correct trajectory. Images show the surface attributes of the performance functional characterize the "basin of attraction/trust region" [12, 13] of this functional which is similar for arbitrary excerpts from the GOTCHA data. Our focusing approach consists of conducting a search procedure with sufficiently small sample intervals to guarantee that at least one sample will fall within the basin of attraction as depicted in Figures 4(a-c).

4.4. Demonstration of a Candidate Solution

An experiment is constructed for reconstructing SAR images by estimating the positions of the antenna during aperture formation using a parametric 3D space curve with only the first 50 pulses every 45 degrees. The search was done using a grid search over candidate trajectories based on the slope coefficients of the space curve where the (X, Y, Z) coefficients can each vary by ± 0.005 with a step size of 0.001. The column entropy function was used to assess the candidate trajectory that will assume a minimum at trajectories that result in coherently focused phase history SAR images. For the entire GOTCHA dataset, the average position error from the estimated trajectory to the ground truth trajectory is $0.0427mm$, $0.0547mm$, and $0.428mm$ for the X, Y, and Z positions respectively. The standard deviation of the position error was $0.0449mm$, $0.048mm$, and $0.0424mm$ for the X, Y, and Z positions respectively. The results for the GOTCHA dataset were consistent for all passes, polarities, and azimuth angles as seen from the example result in Table 1.

5. CONCLUSION

Formation of SAR images requires highly accurate knowledge of the antenna state at the time RF signals are transmitted which is typically obtained using a combination of GPS and INS. SAR dependence on GPS and INS data prohibit SAR image formation in GPS-denied context and this restriction limits the application of this technology. Existing work does not consider the difficult problem of finding antenna trajectories whose relative pose errors fall into the $\epsilon > 2mm.$ regime. Here, we demonstrated that by using the canonical coordinate system that changes to the initial pose parameters that it will shift the focused target phase center, changes to the pose change position parameters greater than $\frac{\lambda}{10}$ cause significant degradation in the focused image, and that by searching for candidate trajectories within the solution space that coherent focused SAR images will be formed.

6. REFERENCES

[1] S. Chen and H. Wang, "SAR target recognition based on deep learning," in *2014 International Conference on Data Science and Advanced Analytics (DSAA)*, 2014, pp. 541–547.

[2] Ryan K. Hersey and Edwin Culpepper, "Radar processing architecture for simultaneous SAR, GMTI, ATR, and tracking," in *2016 IEEE Radar Conference (RadarConf)*. may 2016, IEEE.

[3] J. Zhang, S. Yang, Z. Zhao, and G. Huang, "SAR mapping technology and its application in difficulty terrain area," in *2010 IEEE International Geoscience and Remote Sensing Symposium*, 2010, pp. 3608–3611.

[4] M. Yeremy, J.W.M. Campbell, K. Mattar, and T. Potter, "Ocean surveillance with polarimetric sar," *Canadian Journal of Remote Sensing*, vol. 27, no. 4, pp. 328–344, 2001.

[5] Zbigniew Perski, "Application of SAR imagery and SAR interferometry in digital geological cartography," in *The Current Role of Geological Mapping in Geosciences*, Stanisław R. Ostaficzuk, Ed., Dordrecht, 2005, pp. 225–244, Springer Netherlands.

[6] Andrea Pulella, Rodrigo Aragão Santos, Francescopaolo Sica, Philipp Posovszky, and Paola Rizzoli, "Multi-temporal sentinel-1 backscatter and coherence for rainforest mapping," *Remote Sensing*, vol. 12, no. 5, 2020.

[7] Michael Israel Duersch, *Backprojection for Synthetic Aperture Radar*, Ph.D. thesis, Brigham Young University, 2013.

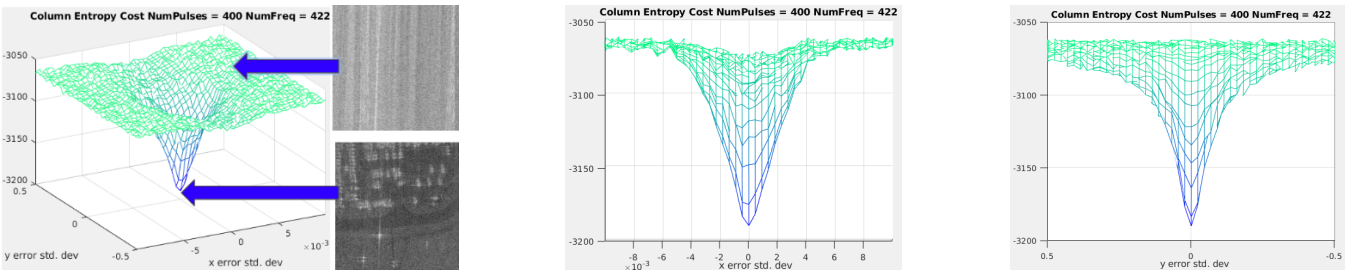

(a) (b) σ_x (c) σ_y

Fig. 4: (a) shows a chart of the column entropy performance functional for trajectories close to the true trajectory. Images are shown within the basin of attraction (focused) and away from it (incoherent). (b,c) show views of the surface basin of attraction for in the canonical x (down-range) and y (cross-range) directions. The trust region curvature dictates sampling interval for the non-linear search to ensure the sample interval is sufficiently small to guarantee that such trust regions are detectable in the search for plausible pose change parameter values.

	Pass 1, HH, 0 Degree	Pass 2, HV, 315 Degree	Pass 5, VH, 225 Degree	Pass 8, VV, 90 Degree
Ground Truth	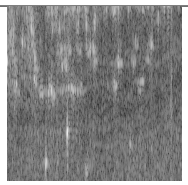	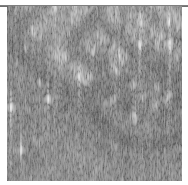	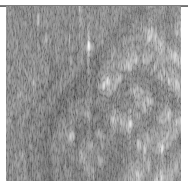	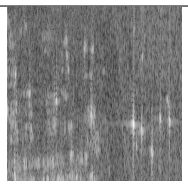
Initial	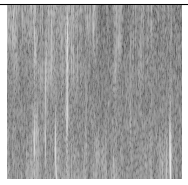	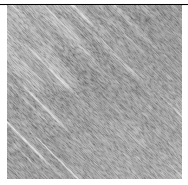	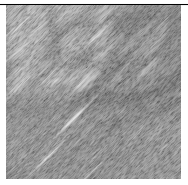	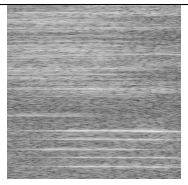
Reconstructed	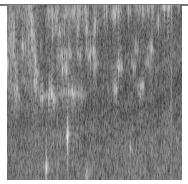	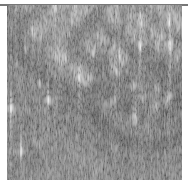	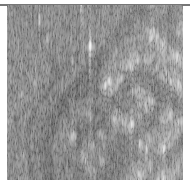	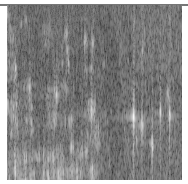

Table 1: Four examples of focused SAR images from the GOTCHA dataset.

[8] Aaron Evers and Julie Ann Jackson, "A comparison of autofocus algorithms for backprojection synthetic aperture radar," in *2020 IEEE International Radar Conference (RADAR)*. apr 2020, IEEE.

[9] "Gotcha volumetric sar data set,version 1.0," Jan. 2021, [Online; Accessed 6-November-2021].

[10] Michael I Duersch and David G Long, "Analysis of time-domain back-projection for stripmap SAR," *International Journal of Remote Sensing*, vol. 36, no. 8, pp. 2010–2036, apr 2015.

[11] Aaron Evers and Julie Ann Jackson, "A generalized phase gradient autofocus algorithm," *IEEE Transactions on Computational Imaging*, vol. 5, no. 4, pp. 606–619, dec 2019.

[12] A.J. Storkey and R. Valabregue, "The basins of attraction of a new hopfield learning rule," *Neural Netw.*, vol. 12, no. 6, pp. 869–876, jul 1999.

[13] J. J. Moré, "Recent developments in algorithms and software for trust region methods," in *Mathematical Programming The State of the Art: Bonn 1982*, pp. 258–287. Springer Berlin Heidelberg, 1983.